Automatica 174 (2025) 112146

Contents lists available at ScienceDirect

Automatica

journal homepage: www.elsevier.com/locate/automatica

Brief Paper

Accelerated secondary frequency regulation and active power sharing for islanded microgrids with external disturbances: A fully distributed approach☆

Boda Ning [a], Qing-Long Han [b,*], Zongyu Zuo [c], Lei Ding [d]

[a] Department of Electrical and Electronic Engineering, Auckland University of Technology, Auckland, 1010, New Zealand
[b] School of Science, Computing and Engineering Technologies, Swinburne University of Technology, Melbourne, VIC 3122, Australia
[c] The Seventh Research Division, Beihang University (BUAA), Beijing 100191, China
[d] Institute of Advanced Technology, Nanjing University of Posts and Telecommunications, Nanjing 210023, China

ARTICLE INFO

Article history:
Received 24 July 2023
Received in revised form 1 October 2024
Accepted 19 December 2024
Available online xxxx

Keywords:
Fully distributed control
Islanded microgrids
Accelerated secondary control
External disturbances

ABSTRACT

Islanded microgrids face some challenges in maintaining stable frequency and sharing proper power among distributed generators (DGs) in the presence of external disturbances. This paper develops a novel fully distributed approach to achieve accelerated secondary frequency regulation (FR) and active power sharing (APS) in islanded microgrids, which enhances system performance and robustness against external disturbances. The proposed control strategy combines advanced consensus algorithms with distributed secondary control loops, eliminating the requirement for a central control unit thereby improving the scalability. Particularly, the fully distributed feature of the proposed control strategy can be understood from two aspects. On one hand, the controller itself is not using global information of (1) communication topology, such as the second smallest eigenvalue of its Laplacian matrix; and (2) the total number of DGs in the microgrid. On the other hand, the estimated settling time is independent of the aforementioned global information. Therefore, the proposed fully distributed control scheme has the potential of becoming a promising solution for the resilient and efficient management of large-scale islanded microgrids. The effectiveness of the designed controllers is validated through numerical examples, demonstrating superior performance in terms of FR, APS, and transient response under various operating conditions.

1. Introduction

In recent years, the importance of microgrids has increased due to the growing demand for reliable and efficient power supply, as well as the integration of renewable energy resources into the power system. Microgrids are small-scale power networks that can operate on their own or in conjunction with the main power grid, providing greater flexibility and resilience (Chen et al., 2017). Islanded microgrids, in particular, have gained attention due to their ability to continue supplying power in the event of a grid outage (Bidram et al., 2014). The primary challenge in islanded microgrid operation is maintaining system stability and power quality, which requires effective strategies for secondary control, such as frequency regulation (FR) and active power sharing (APS) (Guerrero et al., 2011). Conventionally, centralized control methods have been employed to address these issues. For example, a model predictive controller is developed to coordinate parallel operations of inverters in microgrids with saved computational time (Tan et al., 2012). However, centralized control methods suffer from several drawbacks, such as single point of failure, limited scalability, and slow response to external disturbances. To overcome the limitations of centralized methods, researchers have been exploring distributed control approaches for islanded microgrids (Ding et al., 2019; Guo et al., 2015; Simpson-Porco et al., 2015). These approaches are based on the idea that each distributed generator (DG) within the microgrid can autonomously adjust its output according to local measurements and information shared with neighboring DGs. This allows for more robust and scalable control, as well as faster response times to disturbances (Ding et al., 2019; Guo et al., 2015; Simpson-Porco et al., 2015). Agent-based control is a distributed control approach that has been proposed for islanded microgrid management. In this method, each DG is considered as an intelligent agent with the capability to communicate and cooperate with other agents to achieve a common objective, such

☆ The material in this paper was not presented at any conference. This paper was recommended for publication in revised form by Associate Editor Antonella Ferrara under the direction of Editor Thomas Parisini.

* Corresponding author.
E-mail addresses: boda.ning@aut.ac.nz (B. Ning), qhan@swin.edu.au (Q.-L. Han), zzybobby@buaa.edu.cn (Z. Zuo), dl522@163.com (L. Ding).

https://doi.org/10.1016/j.automatica.2025.112146

as balancing the relationship between power supply and load demand (Li et al., 2016). This allows the microgrid to adapt to changes in load demand and generation capacity in a decentralized manner, avoiding the need for a central controller. Another recent advance in distributed control is the use of consensus algorithms, which are designed to enable a group of agents to reach an agreement on certain values or decisions utilizing local information exchange (Dehkordi et al., 2017b). These algorithms have been applied to islanded microgrids for secondary control, leading to improved stability and performance under various operating conditions. For example, a novel secondary frequency restoration controller is proposed considering communication delays in Chen and Guo (2019), where Lyapunov–Krasovskii functions are utilized to analyze the stability of networked DGs.

Finite-time and fixed-time distributed control approaches have emerged as promising methods to address challenges in the control of islanded microgrids, especially in terms of providing fast response times to disturbances and ensuring robust system stability. Both approaches focus on achieving control objectives within short time intervals, which can be advantageous in dynamically changing environments such as islanded microgrids. Specifically, finite-time control algorithms are designed to ensure that control objectives are achieved within a finite time, which can be adjusted according to the desired system performance (Bhat & Bernstein, 2000; Yu & Long, 2015). In the context of islanded microgrids, finite-time algorithms can be employed to provide rapid FR (Xu & Sun, 2018). Moreover, finite-time control approaches can help improve the transient response of islanded microgrids and enhance their resilience to external disturbances, such as sudden changes in load demand or generation capacity. As a variation of finite-time control, fixed-time control ensures that control objectives are achieved within a fixed time interval (Ning et al., 2023). This approach provides better predictability of the system response, as the time required to reach the desired control objectives is upper bounded by a constant, regardless of the initial conditions. Fixed-time control can be advantageous in islanded microgrids, as it ensures that distributed secondary control is achieved within a specific time frame, which leads to improved system stability and power quality, as well as faster recovery from disturbances.

From the aforementioned analysis, accelerated (including finite-time and fixed-time) control approaches are gaining increasing attention in the development of advanced control strategies for islanded microgrids. However, in most of the existing results, controllers are not fully distributed due to the dependence on global information of graphs (Ning et al., 2023). Although some developed accelerated controllers are independent of global information of graphs, the estimated settling time is not explicitly provided (Dehkordi et al., 2017a; Wang et al., 2017; Zuo et al., 2016) or is dependent on global information of graphs (Ning et al., 2021; Zhou et al., 2020). In practice, the communication topology can be time-varying due to the plug-and-play nature of DGs, so it can be extremely difficult to obtain the global topology information especially for large-scale networked DGs. Therefore, how to design a new fully distributed scheme for islanded microgrids, realizing FR and APS with accelerated convergence speed by using fully distributed secondary controllers and the estimated settling time is independent of global information of communication topology and the total number of DGs, is a problem that remains unsolved and challenging, which motivates the current study. The terminology of "fully distributed" has been introduced in Li et al. (2015), where the global information of the entire communication graph is not used in controller design for multi-agent systems.

In this paper, the exploration is concentrated on the challenge of distributed secondary control for islanded microgrids, including both FR and APS, under a scenario where the networked DGs are subject to external disturbances. The main contributions of this paper are summarized as follows. (i) A new fully distributed control strategy is proposed to restore frequencies of DGs in finite-time, while concurrently accomplishing APS among DGs in finite-time. An adaptive control gain is used to adjust the control input of DGs. The adaptive gain-based controller is fully distributed without dependence on global information of communication topology and the total number of DGs; and (ii) A novel fully distributed fixed-time controller is further designed to restore frequencies and realize APS among DGs, under which the derived upper bound of the settling time is independent of the aforementioned global information and the initial deviations caused by primary control. In other words, the controller itself and the estimated settling time are independent of the global information, facilitating the implementing of large-scale networked DGs with preferred performance. Finally, we provide case studies utilizing a modified IEEE 34-bus test system.

2. Preliminaries and problem formulation

2.1. Communication among DGs

Consider an islanded microgrid consisting of n DGs that can communicate with their neighboring DGs via a communication network. The communication existed in the microgrid is modeled by an undirected graph $\mathcal{G} = (\mathcal{V}, \mathcal{E})$, where $\mathcal{V} = \{v_1, v_2, \ldots, v_n\}$ is a vertex set indexed by a DG set $\Omega = \{1, 2, \ldots, n\}$, and $\mathcal{E} = \{(v_i, v_j) \mid v_i, v_j \in \mathcal{V}\}$ is a communication link set. The graph $\mathcal{G}$ can be characterized mathematically by a weighted *adjacency matrix* $\mathcal{A} = [a_{ij}]_{n\times n}$ with $a_{ij} > 0$ if $(v_j, v_i) \in \mathcal{E}$ and $a_{ij} = 0$ otherwise; and a *Laplacian matrix* $L = [l_{ij}]_{n\times n}$ with $l_{ij} = -a_{ij}$ for $i \neq j$, and $l_{ii} = \sum_{j=1}^{n} a_{ij}$. We consider $\mathcal{G}$ is an undirected graph in this paper, i.e., $a_{ij} = a_{ji}$. In distributed secondary control, the ith DG communicates with a neighboring set $\mathcal{N}_i = \{v_j \in \mathcal{V} | (v_i, v_j) \in \mathcal{E}\}$. Meanwhile, the reference level of frequency can be treated as a command sent out from a virtual leader (vertex index 0), which is received by a few (but not all) DGs. Let $\bar{\mathcal{G}}$ be the communication graph among n DGs and the virtual leader. Note that the virtual leader only sends out the reference level but does not receive any information from other DGs. If the ith DG receives the information from the leader, an indicator b_i is set to be a positive value, i.e., $b_i > 0$; and $b_i = 0$ otherwise. Let $H = L+B$ with $B = \text{diag}\{b_1, b_2, \ldots, b_n\}$. Denote $\lambda_2(L)$ and $\lambda_{\min}(H)$ as the second smallest eigenvalue and the smallest eigenvalue of L and H, respectively, which provide useful information about the graph's structure and properties.

2.2. Primary and secondary control for microgrids

A typical DG unit consists of a DC source, an LC filter, a voltage-controlled voltage source inverter and an RL output connector. In Fig. 1, a block diagram illustrates the control structure for the ith DG. Droop control is utilized in the primary control layer to maintain the frequency stability, i.e., for the ith DG,

$$\omega_i = \omega_i^* - m_i P_i, \tag{1}$$

$$v_{\text{mag},i}^* = V_i^* - \kappa_i Q_i, \tag{2}$$

where ω_i^* and V_i^* are primary control references for the ith DG that are produced in the secondary control layer; ω_i and $v_{\text{mag},i}^*$ are the angular frequency and the output voltage magnitude of the ith DG, respectively; P_i and Q_i are the active and reactive power of the ith DG, respectively; m_i and κ_i are some droop coefficients for the ith DG. Note that the objective of frequency control is to

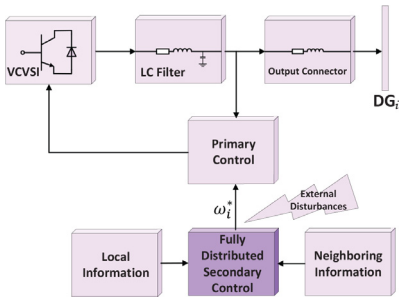

Fig. 1. A fully distributed control block diagram for inverter-based DG *i*.

design a proper ω_i^* such that ω_i is synchronized to a reference level, ω_r.

Considering physical components, the nonlinear dynamics for the *i*th DG is provided in Bidram et al. (2013), Zuo et al. (2016). Then, applying the feedback linearization and considering that DGs operate in noisy circumstances, the dynamics of frequency and active power for DG *i*, including input disturbances, can be characterized as (Zhao et al., 2021)

$$\dot{\omega}_i = u_i^{\omega} + \zeta_i^{\omega}, \tag{3}$$

$$m_i \dot{P}_i = u_i^{P}, \tag{4}$$

where ζ_i^{ω} can be external disturbances, while u_i^{ω} and u_i^{P} are control inputs to be designed, of frequency and active power, respectively. As a result, ω_i^* can be calculated as

$$\omega_i^* = \int \left(u_i^{\omega} + u_i^{P} + \zeta_i^{\omega}\right) \mathrm{d}t. \tag{5}$$

It is recognized that a distributed control approach offers superior benefits compared to a centralized method, particularly in terms of microgrid scalability and reliability enhancement. Consequently, our objective is to develop distributed secondary controllers u_i^{ω} and u_i^{P} utilizing data from neighboring DGs, facilitated by a communication network.

2.3. Problem formulation

A fully distributed secondary control strategy for islanded microgrids in this paper indicates that utilization of global topology information is avoided such as the second smallest eigenvalue of the Laplacian matrix of communication topology. Meanwhile, we are dealing with secondary control with accelerated convergence, and the controllers (and the estimated settling time in the fixed-time case) should not depend on global topology information and the total number of DGs to reflect the fully distributed feature of the proposed control scheme.

Therefore, the problem to be addressed is stated as: for the system (3)–(4), design fully distributed controllers $u_i^{\omega}(t)$ and $u_i^{P}(t)$ without using global topology information, $i \in \Omega$,

(1) to realize practical finite-time FR and APS among *n* DGs, respectively, i.e.,

$$\begin{cases} \lim_{t\to T} |\omega_i(t) - \omega_r| \le \delta; \\ |\omega_i(t) - \omega_r| \le \delta, \forall t \ge T, \forall i \in \Omega, \end{cases}$$

and

$$\begin{cases} \lim_{t\to T} |m_i P_i(t) - m_j P_j(t)| \le \delta; \\ |m_i P_i(t) - m_j P_j(t)| \le \delta, \forall t \ge T, \forall i, j \in \Omega, \end{cases}$$

where δ is a positive adjustable constant, T is upper bounded by a finite time; or

(2) to realize practical fixed-time FR and APS among *n* DGs, respectively, i.e.,

$$\begin{cases} \lim_{t\to T} |\omega_i(t) - \omega_r| \le \delta; \\ |\omega_i(t) - \omega_r| \le \delta, \forall t \ge T, \forall i \in \Omega, \end{cases}$$

and

$$\begin{cases} \lim_{t\to T} |m_i P_i(t) - m_j P_j(t)| \le \delta; \\ |m_i P_i(t) - m_j P_j(t)| \le \delta, \forall t \ge T, \forall i, j \in \Omega, \end{cases}$$

where T is upper bounded by a fixed time that is independent of initial states and global topology information.

Next, some mild assumptions are made for the considered microgrids.

Assumption 1. The undirected graph $\mathcal{G}$ corresponding to *n* DGs is connected. And at least one DG can access the frequency reference level.

Assumption 2. The external disturbances are bounded. Specifically, $|\zeta_i^{\omega}(t)| \le d$, where d is a known constant.

2.4. Practical finite/fixed-time stability

Consider a nonlinear system

$$\dot{x}(t) = f(x(t)), x_0 = x(0), \tag{6}$$

where $x \in \mathbb{R}^n$ is the state, $f(x(t)) : \mathbb{R}^n \to \mathbb{R}^n$ is a nonlinear function. The following two preliminary lemmas are provided.

Lemma 1 (Zhu et al., 2011)**.** *Suppose there exists a continuous positive definite function $V(x)$ for system (6) such that*

$$\dot{V}(x) \le -\alpha V^a(x) + \eta,$$

where $\alpha > 0$, $0 < a < 1$, and $0 < \eta < \infty$. Then, system (6) is practical finite-time stable. Specifically, the state of the system is bounded in finite time in the set of

$$\Phi_1 \triangleq \left\{ x \middle| V^a(x) \le \frac{\eta}{\alpha(1-\varepsilon)} \right\},$$

where $0 < \varepsilon < 1$. And the finite time T_1 to reach the set Φ_1 is bounded by

$$T_1 \le \frac{V^{1-a}(x_0)}{\alpha\varepsilon(1-a)}$$

with x_0 being the initial state.

Lemma 2. *Suppose there exists a continuous positive definite function $V(x)$ for system (6) such that*

$$\dot{V}(x) \le -\alpha V^{1-\psi}(x) - \beta V^{1+\psi}(x) + \eta,$$

where $\alpha, \beta > 0$, $0 < \psi < 1$, and $0 < \eta < \infty$. Then, system (6) is practical fixed-time stable. Specifically, the state of the system is bounded in fixed time in the set of

$$\Phi_2 \triangleq \left\{ x \middle| V(x) \le \frac{\eta}{2(1-\varepsilon)\sqrt{\alpha\beta}} \right\},$$

where $0 < \varepsilon < 1$. And the fixed time T_2 to reach the set Φ_2 is bounded by

$$T_2 \le \frac{\pi}{2\psi\varepsilon\sqrt{\alpha\beta}}.$$

Proof. The proof procedure is similar to that in Cao et al. (2020). A sketch of the proof is provided in what follows. First, we need to rewrite $\dot{V}(x)$ as

$$\dot{V}(x) \le -\alpha V^{1-\psi}(x) - \beta V^{1+\psi}(x) + \eta$$

$$
\begin{aligned}
&= -\alpha\varepsilon V^{1-\psi}(x) - \alpha(1-\varepsilon)V^{1-\psi}(x) \\
&\quad - \beta\varepsilon V^{1+\psi}(x) - \beta(1-\varepsilon)V^{1+\psi}(x) + \eta \\
&\le -\alpha\varepsilon V^{1-\psi}(x) - \beta\varepsilon V^{1+\psi}(x) - 2(1-\varepsilon)\sqrt{\alpha\beta}V(x) + \eta,
\end{aligned}
$$

then the proof can be completed by using Lemma 2.1 in Ning et al. (2018) and the comparison principle.

Lemma 3 (*Krstic et al., 1995*). *$\forall x, y \in R$, the following inequality holds*

$$xy \le \frac{c^p}{p}|x|^p + \frac{1}{qc^q}|y|^q,$$

where $c > 0$, $p > 1$, $q > 1$, and $(p-1)(q-1) = 1$.

3. Fully distributed finite-time FR and APS

In order to achieve FR for DGs, a fully distributed controller is designed for DG i, $i \in \Omega$, as:

$$
\begin{aligned}
u_i^{\omega} = &-\mu_i\alpha\text{sign}\Big(\sum_{j\in\mathcal{N}_i} a_{ij}(\omega_i-\omega_j) + b_i(\omega_i-\omega_{\text{r}})\Big) \\
&- k_1\text{sign}\Big(\sum_{j\in\mathcal{N}_i} a_{ij}(\omega_i-\omega_j) + b_i(\omega_i-\omega_{\text{r}})\Big),
\end{aligned} \tag{7}
$$

$$\dot{\mu}_i = \alpha\Big|\sum_{j\in\mathcal{N}_i} a_{ij}(\omega_i-\omega_j) + b_i(\omega_i-\omega_{\text{r}})\Big| - \alpha\mu_i, \tag{8}$$

where μ_i is an adaptive gain with $\mu_i(0) > 0$, $\alpha > 0$, and $k_1 \ge d$.

In order to realize APS, a fully distributed controller is further proposed for DG i, $i \in \Omega$, as:

$$u_i^{P} = -\alpha\text{sign}\Big(\sum_{j\in\mathcal{N}_i} a_{ij}\nu_{ij}(m_iP_i - m_jP_j)\Big), \tag{9}$$

$$\dot{\nu}_{ij} = \frac{\alpha}{2}a_{ij}|m_iP_i - m_jP_j| - \frac{\alpha}{2}\nu_{ij}, \tag{10}$$

where ν_{ij} is an adaptive gain with $\nu_{ij} = \nu_{ji}$ and $\nu_{ij}(0) > 0$. Denote $e = [e_1, e_2, \ldots, e_n]^T$ and $\epsilon = [\epsilon_1, \epsilon_2, \ldots, \epsilon_n]^T$, where $e_i = \omega_i - \omega_{\text{r}}$, $i = 1, 2, \ldots, n$, and

$$\epsilon_i = m_iP_i - \frac{\sum_{i=1}^n m_iP_i}{n}. \tag{11}$$

Let $\hat{\mathcal{G}}$ denote an undirected graph with an adjacency matrix $\hat{\mathcal{A}} = [a_{ij}^2]_{n\times n}$. Let $\hat{L}$ denote the Laplacian matrix of graph $\hat{\mathcal{G}}$. Construct two non-negative functions of

$$V_1 = \frac{1}{4}\sum_{i=1}^n\sum_{j\in\mathcal{N}_i} a_{ij}(e_i-e_j)^2 + \frac{1}{2}\sum_{i=1}^n b_ie_i^2 + \frac{1}{2}\sum_{i=1}^n(\mu_i-\theta_1)^2, \tag{12}$$

and

$$V_2 = \frac{1}{2}\sum_{i=1}^n \epsilon_i^2 + \frac{1}{2}\sum_{i=1}^n\sum_{j=1}^n(\nu_{ij}-\theta_2)^2, \tag{13}$$

where $\theta_1 = 1/\sqrt{2\lambda_{\min}(H)}$ and $\theta_2 = 1/\sqrt{\lambda_2(\hat{L})}$.

Theorem 1. *Under Assumptions 1 and 2, for the system described by (3) and (4), by using fully distributed controllers described by (7)–(10), practical finite-time FR and APS are achieved. Specifically, the FR error and the APS error converge into the set of*

$$\Omega_1^e \triangleq \left\{e \middle| e^Te \le \frac{2}{\lambda_{min}(H)}\left(\frac{n\theta_1^2(\lambda_{min}(H)+1)}{2(1-\varepsilon_1)}\right)^2\right\},$$

and

$$\Omega_2^{\epsilon} \triangleq \left\{\epsilon \middle| \epsilon^T\epsilon \le 2\left(\frac{n^2\theta_2^2(2\lambda_2(\hat{L})+1)}{4(1-\varepsilon_2)}\right)^2\right\},$$

respectively, where $0 < \varepsilon_1, \varepsilon_2 < 1$. And the finite time T_1^* and T_2^* to reach Ω_1^e and Ω_2^{ϵ} are bounded by

$$T_1^* \le \frac{2\sqrt{V_1(0)}}{\alpha\varepsilon_1}, \tag{14}$$

and

$$T_2^* \le \frac{2\sqrt{V_2(0)}}{\alpha\varepsilon_2}, \tag{15}$$

respectively.

Proof. Since $e_i = \omega_i - \omega_{\text{r}}$, using (3) and (7), the time derivative of e_i can be calculated as

$$
\begin{aligned}
\dot{e}_i = &-\mu_i\alpha\text{sign}\Big(\sum_{j\in\mathcal{N}_i} a_{ij}(e_i-e_j) + b_ie_i\Big) \\
&- k_1\text{sign}\Big(\sum_{j\in\mathcal{N}_i} a_{ij}(e_i-e_j) + b_ie_i\Big) + \zeta_i^{\omega}.
\end{aligned}
$$

From (12), the time derivative of V_1 can be calculated as

$$\dot{V}_1 = \sum_{i=1}^n \dot{e}_i\Big(\sum_{j\in\mathcal{N}_i} a_{ij}(e_i-e_j) + b_ie_i\Big) + \sum_{i=1}^n \dot{\mu}_i(\mu_i-\theta_1).$$

Let $z_i = \sum_{j\in\mathcal{N}_i} a_{ij}(e_i-e_j) + b_ie_i$ and $\mu_{i,1} = \mu_i - \theta_1$, $i = 1, 2, \ldots, n$. Then, one obtains that

$$
\begin{aligned}
\dot{V}_1 &= -\alpha\sum_{i=1}^n \mu_i|z_i| - k_1\sum_{i=1}^n|z_i| + \sum_{i=1}^n \zeta_i^{\omega}z_i \\
&\quad + \alpha\sum_{i=1}^n \mu_{i,1}|z_i| - \alpha\sum_{i=1}^n \mu_{i,1}\mu_i \\
&\le -\alpha\theta_1\sum_{i=1}^n|z_i| - \alpha\sum_{i=1}^n \mu_{i,1}\mu_i \\
&= -\alpha\theta_1\sum_{i=1}^n|z_i| - \alpha\theta_1\sum_{i=1}^n\Big(\lambda_{\min}(H)\mu_{i,1}^2\Big)^{\frac{1}{2}} \\
&\quad + \alpha\theta_1\sum_{i=1}^n\Big(\lambda_{\min}(H)\mu_{i,1}^2\Big)^{\frac{1}{2}} - \alpha\sum_{i=1}^n \mu_{i,1}\mu_i,
\end{aligned} \tag{16}
$$

where the fact that $k_1\sum_{i=1}^n|z_i| \ge \sum_{i=1}^n \zeta_i^{\omega}z_i$ due to $k_1 \ge d$ under Assumption 2 has been used to get the inequality. It can be further verified that

$$
\begin{aligned}
&\alpha\theta_1\sum_{i=1}^n\Big(\lambda_{\min}(H)\mu_{i,1}^2\Big)^{\frac{1}{2}} - \alpha\sum_{i=1}^n \mu_{i,1}\mu_i \\
\le&\frac{\alpha}{2}\sum_{i=1}^n\Big(\theta_1^2\lambda_{\min}(H) + \mu_{i,1}^2\Big) - \alpha\sum_{i=1}^n \mu_{i,1}\Big(\mu_{i,1}+\theta_1\Big) \\
\le&\frac{\alpha}{2}\sum_{i=1}^n\Big(\theta_1^2\lambda_{\min}(H) + \mu_{i,1}^2\Big) - \alpha\sum_{i=1}^n\Big(\mu_{i,1}^2 - \frac{1}{2}\mu_{i,1}^2 - \frac{1}{2}\theta_1^2\Big) \\
=&\frac{\alpha n\theta_1^2(\lambda_{\min}(H)+1)}{2} \triangleq \Pi_1.
\end{aligned}
$$

Thus, (16) can be further calculated as

$$\begin{aligned}\dot{V}_1 &\le -\alpha\theta_1\sum_{i=1}^{n}|z_i| - \alpha\theta_1\sum_{i=1}^{n}\left(\lambda_{\min}(H)\mu_{i,1}^2\right)^{\frac{1}{2}} + \Pi_1\\ &\le -\alpha\theta_1\left(\sum_{i=1}^{n}\left(z_i^2 + \lambda_{\min}(H)\mu_{i,1}^2\right)\right)^{\frac{1}{2}} + \Pi_1\\ &\le -\alpha\theta_1\left(2\lambda_{\min}(H)V_1\right)^{\frac{1}{2}} + \Pi_1.\end{aligned}$$

Since $\theta_1 = 1/\sqrt{2\lambda_{\min}(H)}$, by using Lemma 1, one can obtain that the frequency of DGs, $\omega = [\omega_1, \omega_2, \ldots, \omega_n]^T$, converges into the set of

$$\Omega_1 = \left\{\omega \middle| V_1 \le \left(\frac{\Pi_1}{\alpha(1-\varepsilon_1)}\right)^2\right\}$$

in finite time T_1^* bounded by

$$T_1^* \le \frac{2\sqrt{V_1(0)}}{\alpha\varepsilon_1}.$$

Note that

$$V_1 \ge \frac{1}{2}e^THe \ge \frac{1}{2}\lambda_{\min}(H)e^Te,$$

so from the set Ω_1, one further obtains that the FR error converges into the set of

$$\Omega_1^e = \left\{e \middle| e^Te \le \frac{2}{\lambda_{\min}(H)}\left(\frac{\Pi_1}{\alpha(1-\varepsilon_1)}\right)^2\right\}$$

in finite time T_1^*. From the above analysis, we can conclude that practical finite-time FR is achieved for DGs by using fully distributed controller (7)–(8). Next, we prove that practical finite-time APS is realized among DGs.

From (4), (9) and (11), the time derivative of ϵ_i can be calculated as

$$\dot{\epsilon}_i = -\nu_i\alpha\,\mathrm{sign}\left(\sum_{j\in\mathcal{N}_i}a_{ij}(\epsilon_i - \epsilon_j)\right).$$

Then, from (13), the time derivative of V_2 can be calculated as

$$\dot{V}_2 = \sum_{i=1}^{n}\epsilon_i\dot{\epsilon}_i + \sum_{i=1}^{n}\sum_{j=1}^{n}\dot{\nu}_{ij}(\nu_{ij} - \theta_2).$$

Let $\nu_{i,2} = \nu_{ij} - \theta_2$, $i = 1, 2, \ldots, n$. Then, one obtains that

$$\begin{aligned}\dot{V}_2 &= \sum_{i=1}^{n}\epsilon_i\dot{\epsilon}_i + \sum_{i=1}^{n}\sum_{j=1}^{n}\dot{\nu}_{ij}(\nu_{ij} - \theta_2)\\ &= -\alpha\sum_{i=1}^{n}\epsilon_i\,\mathrm{sign}\left(\sum_{j=1}^{n}a_{ij}\nu_{ij}(\epsilon_i - \epsilon_j)\right)\\ &\quad + \sum_{i=1}^{n}\sum_{j=1}^{n}\nu_{i,2}\left(\frac{\alpha}{2}a_{ij}|m_iP_i - m_jP_j| - \frac{\alpha}{2}\nu_{ij}\right)\\ &= -\frac{\alpha}{2}\sum_{i=1}^{n}\sum_{j=1}^{n}a_{ij}\nu_{ij}|\epsilon_i - \epsilon_j|\\ &\quad + \sum_{i=1}^{n}\sum_{j=1}^{n}\nu_{i,2}\left(\frac{\alpha}{2}a_{ij}|\epsilon_i - \epsilon_j| - \frac{\alpha}{2}\nu_{ij}\right)\\ &= -\frac{\alpha\theta_2}{2}\sum_{i=1}^{n}\sum_{j=1}^{n}a_{ij}|\epsilon_i - \epsilon_j| - \frac{\alpha\theta_2}{2}\sum_{i=1}^{n}\sum_{j=1}^{n}\left(2\lambda_2(\hat{L})\nu_{i,2}^2\right)^{\frac{1}{2}}\\ &\quad + \frac{\alpha\theta_2}{2}\sum_{i=1}^{n}\sum_{j=1}^{n}\left(2\lambda_2(\hat{L})\nu_{i,2}^2\right)^{\frac{1}{2}} - \frac{\alpha}{2}\sum_{i=1}^{n}\sum_{j=1}^{n}\nu_{i,2}\nu_{ij}. \qquad (17)\end{aligned}$$

It can be verified that

$$\begin{aligned}&\alpha\theta_2\left(2\lambda_2(\hat{L})\nu_{i,2}^2\right)^{\frac{1}{2}} - \alpha\nu_{i,2}\nu_{ij}\\ \le&\frac{\alpha}{2}\left(2\theta_2^2\lambda_2(\hat{L}) + \nu_{i,2}^2\right) - \alpha\nu_{i,2}\left(\nu_{i,2} + \theta_2\right)\\ \le&\frac{\alpha}{2}\left(2\theta_2^2\lambda_2(\hat{L}) + \nu_{i,2}^2\right) - \alpha\left(\nu_{i,2}^2 - \frac{1}{2}\nu_{i,2}^2 - \frac{1}{2}\theta_2^2\right)\\ =&\frac{\alpha}{2}\left(2\theta_2^2\lambda_2(\hat{L}) + \theta_2^2\right).\end{aligned}$$

Let $\Pi_2 = \frac{\alpha n^2\theta_2^2(2\lambda_2(\hat{L})+1)}{4}$. Then, (17) can be further calculated as

$$\begin{aligned}\dot{V}_2 &\le -\frac{\alpha\theta_2}{2}\sum_{i=1}^{n}\sum_{j=1}^{n}a_{ij}|\epsilon_i - \epsilon_j| - \frac{\alpha\theta_2}{2}\sum_{i=1}^{n}\sum_{j=1}^{n}\left(2\lambda_2(\hat{L})\nu_{i,2}^2\right)^{\frac{1}{2}} + \Pi_2\\ &\le -\frac{\alpha\theta_2}{2}\left(\sum_{i=1}^{n}\sum_{j=1}^{n}\left(a_{ij}^2(\epsilon_i - \epsilon_j)^2 + 2\lambda_2(\hat{L})\nu_{i,2}^2\right)\right)^{\frac{1}{2}} + \Pi_2\\ &\le -\frac{\alpha\theta_2}{2}\left(4\lambda_2(\hat{L})V_2\right)^{\frac{1}{2}} + \Pi_2 = -\alpha\theta_2\left(\lambda_2(\hat{L})V_2\right)^{\frac{1}{2}} + \Pi_2,\end{aligned}$$

where the fact that $\sum_{i=1}^{n}\sum_{j=1}^{n}a_{ij}^2(\epsilon_i - \epsilon_j)^2 \ge 2\epsilon^T\hat{L}\epsilon \ge 2\lambda_2(\hat{L})\epsilon^T\epsilon$ has been used to get the last inequality. Since $\theta_2 = 1/\sqrt{\lambda_2(\hat{L})}$, by using Lemma 1, one can obtain that the APS of DGs, $P = [m_1P_1, m_2P_2, \ldots, m_nP_n]^T$, converges into the set of

$$\Omega_2 = \left\{P \middle| V_2 \le \left(\frac{\Pi_2}{\alpha(1-\varepsilon_2)}\right)^2\right\}$$

in finite time T_2^* bounded by

$$T_2^* \le \frac{2\sqrt{V_2(0)}}{\alpha\varepsilon_2}.$$

Note that

$$V_2 \ge \frac{1}{2}\epsilon^T\epsilon,$$

so from the set Ω_2, one further obtains that the APS error converges into the set of

$$\Omega_2^\epsilon = \left\{\epsilon \middle| \epsilon^T\epsilon \le 2\left(\frac{\Pi_2}{\alpha(1-\varepsilon_2)}\right)^2\right\}$$

in finite time T_2^*. Hence, practical finite-time APS is realized among DGs by using fully distributed controller (9)–(10).

4. Fully distributed fixed-time FR and APS

The settling time estimation of (14) and (15) in Theorem 1 depends on initial conditions of all DGs, which can be difficult to obtain in practice, particularly for a large-scale networked DGs. To further remove this restriction, fully distributed fixed-time controllers are proposed in this section.

In order to achieve FR for DGs, a fully distributed controller is designed for DG i, $i \in \Omega$, as:

$$\begin{aligned}u_i^\omega = &-\bar{\mu}_i\alpha\,\mathrm{sig}^{1-\xi}\left(\sum_{j\in\mathcal{N}_i}a_{ij}(\omega_i - \omega_j) + b_i(\omega_i - \omega_r)\right)\\ &-\bar{\mu}_i\alpha\,\mathrm{sig}^{1+\xi}\left(\sum_{j\in\mathcal{N}_i}a_{ij}(\omega_i - \omega_j) + b_i(\omega_i - \omega_r)\right)\\ &-k_2\,\mathrm{sign}\left(\sum_{j\in\mathcal{N}_i}a_{ij}(\omega_i - \omega_j) + b_i(\omega_i - \omega_r)\right), \qquad (18)\end{aligned}$$

$$\dot{\bar{\mu}}_i = \alpha\left|\sum_{j\in\mathcal{N}_i} a_{ij}(\omega_i-\omega_j)+b_i(\omega_i-\omega_{\rm r})\right|^{2-\xi} + \alpha\left|\sum_{j\in\mathcal{N}_i} a_{ij}(\omega_i-\omega_j)+b_i(\omega_i-\omega_{\rm r})\right|^{2+\xi} - \alpha\bar{\mu}_i - \alpha h\bar{\mu}_i^5, \tag{19}$$

where $\bar{\mu}_i$ is an adaptive gain with $\bar{\mu}_i(0)>0$, $0<\xi<1$, $k_2\geq d$, and $h>1$.

In order to realize APS, a fully distributed controller is further proposed for DG i, $i\in\Omega$, as:

$$u_i^P = -\alpha\sum_{j\in\mathcal{N}_i} a_{ij}\bar{v}_{ij}\mathrm{sig}^{1-\xi}(m_iP_i-m_jP_j) - \alpha\sum_{j\in\mathcal{N}_i} a_{ij}\bar{v}_{ij}\mathrm{sig}^{1+\xi}(m_iP_i-m_jP_j), \tag{20}$$

$$\dot{\bar{v}}_{ij} = \frac{\alpha}{2}a_{ij}|m_iP_i-m_jP_j|^{2-\xi} + \frac{\alpha}{2}a_{ij}|m_iP_i-m_jP_j|^{2+\xi} - \frac{\alpha}{2}\bar{v}_{ij} - \frac{\alpha}{2}h\bar{v}_{ij}^5, \tag{21}$$

where $\bar{v}_{ij}$ is an adaptive gain with $\bar{v}_{ij}=\bar{v}_{ji}$ and $\bar{v}_i(0)>0$.

Let $\bar{\mathcal{G}}$ and $\tilde{\mathcal{G}}$ denote undirected graphs with adjacency matrices $\bar{\mathcal{A}}=[a_{ij}^{\frac{2}{2-\xi}}]_{n\times n}$ and $\tilde{\mathcal{A}}=[a_{ij}^{\frac{2}{2+\xi}}]_{n\times n}$, respectively, and the corresponding Laplacian matrices are $\bar{L}$ and $\tilde{L}$, respectively. Denote $\underline{\lambda}_2=\min\{\lambda_2(\bar{L}),\lambda_2(\tilde{L})\}$. Construct two non-negative functions of

$$V_3 = \frac{1}{4}\sum_{i=1}^n\sum_{j\in\mathcal{N}_i} a_{ij}(e_i-e_j)^2 + \frac{1}{2}\sum_{i=1}^n b_ie_i^2 + \frac{1}{2}\sum_{i=1}^n(\bar{\mu}_i-\theta_3)^2, \tag{22}$$

and

$$V_4 = \frac{1}{2}\sum_{i=1}^n\epsilon_i^2 + \frac{1}{2}\sum_{i=1}^n\sum_{j=1}^n(\bar{v}_{ij}-\theta_4)^2, \tag{23}$$

where $\theta_3=(2n)^{\frac{\xi}{4}}/(2\lambda_{\min}(H))$ and $\theta_4=(2n^2)^{\frac{\xi}{4}}/(2\underline{\lambda}_2)$. Let

$$\bar{\Pi}_3 \triangleq \frac{(h\theta_3^5+\theta_3)^2}{20h^2\theta_3^4} + \frac{5^5(5h\theta_3)^6}{6(6(h-1))^5} + \frac{3^3(10h\theta_3^3)^4}{4(40h\theta_3^2)^3} + \frac{1}{2}\theta_3^2\lambda_{\min}^{2-\xi}(H) + \frac{1}{2}\theta_3^2\lambda_{\min}^{2+\xi}(H),$$

and

$$\bar{\Pi}_4 \triangleq \frac{(h\theta_4^5+\theta_4)^2}{20h^2\theta_4^4} + \frac{5^5(5h\theta_4)^6}{6(6(h-1))^5} + \frac{3^3(10h\theta_4^3)^4}{4(40h\theta_4^2)^3} + \frac{1}{2}\theta_4^2 2^{2-\xi}\lambda_2^{2-\xi}(\bar{L}) + \frac{1}{2}\theta_4^2 2^{2+\xi}\lambda_2^{2+\xi}(\tilde{L}).$$

Theorem 2. *Under Assumptions 1 and 2, for the system described by (3) and (4), by using fully distributed controllers described by (18)–(21), practical fixed-time FR and APS are achieved. Specifically, the FR error and the APS error converge into the set of*

$$\Omega_3^e \triangleq \left\{e\left|e^Te\leq\frac{n\bar{\Pi}_3}{\lambda_{min}(H)(1-\varepsilon_3)}\right.\right\},$$

and

$$\Omega_4^\epsilon \triangleq \left\{\epsilon\left|\epsilon^T\epsilon\leq\frac{n^2\bar{\Pi}_4}{2(1-\varepsilon_4)}\right.\right\},$$

respectively, where e and ϵ are defined in Section 3, $0<\varepsilon_3,\varepsilon_4<1$. And the fixed time T_3^* and T_4^* to reach Ω_3^e and Ω_4^ϵ are bounded by

$$T_3^*\leq\frac{\pi}{\varepsilon_3\xi\alpha}, \tag{24}$$

and

$$T_4^*\leq\frac{\pi}{\varepsilon_4\xi\alpha}, \tag{25}$$

respectively.

Proof. Let $\bar{\mu}_{i,3}=\bar{\mu}_i-\theta_3$, $i=1,2,\ldots,n$. From (22), the time derivative of V_3 can be calculated as

$$\begin{aligned}\dot{V}_3 &= -\alpha\sum_{i=1}^n\bar{\mu}_i|z_i|^{2-\xi} - \alpha\sum_{i=1}^n\bar{\mu}_i|z_i|^{2+\xi} - k_2\sum_{i=1}^n|z_i| + \sum_{i=1}^n\zeta_i^\omega z_i + \alpha\sum_{i=1}^n\bar{\mu}_{i,3}|z_i|^{2-\xi} + \alpha\sum_{i=1}^n\bar{\mu}_{i,3}|z_i|^{2+\xi} - \alpha\sum_{i=1}^n\bar{\mu}_{i,3}(\bar{\mu}_i+h\bar{\mu}_i^5)\\ &\leq -\alpha\theta_3\sum_{i=1}^n|z_i|^{2-\xi} - \alpha\theta_3\sum_{i=1}^n|z_i|^{2+\xi} - \alpha\sum_{i=1}^n\bar{\mu}_{i,3}(\bar{\mu}_i+h\bar{\mu}_i^5)\\ &= -\alpha\theta_3\sum_{i=1}^n|z_i|^{2-\xi} - \alpha\theta_3\sum_{i=1}^n\left(\lambda_{\min}(H)\bar{\mu}_{i,3}^2\right)^{\frac{2-\xi}{2}} + \alpha\theta_3\sum_{i=1}^n\left(\lambda_{\min}(H)\bar{\mu}_{i,3}^2\right)^{\frac{2-\xi}{2}} - \alpha\theta_3\sum_{i=1}^n|z_i|^{2+\xi}\\ &\quad - \alpha\theta_3\sum_{i=1}^n\left(\lambda_{\min}(H)\bar{\mu}_{i,3}^2\right)^{\frac{2+\xi}{2}} + \alpha\theta_3\sum_{i=1}^n\left(\lambda_{\min}(H)\bar{\mu}_{i,3}^2\right)^{\frac{2+\xi}{2}} - \alpha\sum_{i=1}^n\bar{\mu}_{i,3}(\bar{\mu}_i+h\bar{\mu}_i^5).\end{aligned} \tag{26}$$

where $k_2\geq d$ under Assumption 2 has been used to get the inequality. Note that

$$\begin{aligned}&\frac{1}{2}\left(\theta_3^2\lambda_{\min}^{2-\xi}(H)+\bar{\mu}_{i,3}^{2(2-\xi)}\right)+\frac{1}{2}\left(\theta_3^2\lambda_{\min}^{2+\xi}(H)+\bar{\mu}_{i,3}^{2(2+\xi)}\right) - \bar{\mu}_{i,3}(\bar{\mu}_{i,3}+\theta_3) - \bar{\mu}_{i,3}h(\bar{\mu}_{i,3}+\theta_3)^5\\ =&\frac{1}{2}\theta_3^2\lambda_{\min}^{2-\xi}(H)+\frac{1}{2}\bar{\mu}_{i,3}^{2(2-\xi)}+\frac{1}{2}\theta_3^2\lambda_{\min}^{2+\xi}(H)+\frac{1}{2}\bar{\mu}_{i,3}^{2(2+\xi)} - h\bar{\mu}_{i,3}^6 - 5h\theta_3\bar{\mu}_{i,3}^5 - 10h\theta_3^2\bar{\mu}_{i,3}^4 - 10h\theta_3^3\bar{\mu}_{i,3}^3 - (5h\theta_3^4+1)\bar{\mu}_{i,3}^2 - (h\theta_3^5+\theta_3)\bar{\mu}_{i,3}\\ \leq&-5h\theta_3^4\bar{\mu}_{i,3}^2+\frac{c_1^2}{2}\bar{\mu}_{i,3}^2+\frac{1}{2c_1^2}(h\theta_3^5+\theta_3)^2 + \frac{1}{2}\bar{\mu}_{i,3}^2(\bar{\mu}_{i,3}^{2-2\xi}-\bar{\mu}_{i,3}^4-1)+\frac{1}{2}\bar{\mu}_{i,3}^2(\bar{\mu}_{i,3}^{2+2\xi}-\bar{\mu}_{i,3}^4-1) - (h-1)\bar{\mu}_{i,3}^6+\frac{5c_2^{\frac{6}{5}}}{6}\bar{\mu}_{i,3}^6+\frac{1}{6}\left(\frac{5h\theta_3}{c_2}\right)^6 - 10h\theta_3^2\bar{\mu}_{i,3}^4+\frac{3c_3^{\frac{4}{3}}}{4}\bar{\mu}_{i,3}^4+\frac{1}{4}\left(\frac{10h\theta_3^3}{c_3}\right)^4 + \frac{1}{2}\theta_3^2\lambda_{\min}^{2-\xi}(H)+\frac{1}{2}\theta_3^2\lambda_{\min}^{2+\xi}(H)\\ =&\frac{(h\theta_3^5+\theta_3)^2}{20h^2\theta_3^4}+\frac{5^5(5h\theta_3)^6}{6(6(h-1))^5}+\frac{3^3(10h\theta_3^3)^4}{4(40h\theta_3^2)^3} + \frac{1}{2}\theta_3^2\lambda_{\min}^{2-\xi}(H)+\frac{1}{2}\theta_3^2\lambda_{\min}^{2+\xi}(H)=\bar{\Pi}_3,\end{aligned}$$

where Lemma 3 has been used to get the inequality, and the selection of

$$\begin{cases} c_1 &= h\theta_3^2\sqrt{10}, \\ c_2 &= (\frac{6}{5}(h-1))^{\frac{5}{6}}, \\ c_3 &= (\frac{40h\theta_3^2}{3})^{\frac{3}{4}} \end{cases}$$

has been utilized to obtain the last equality. Therefore, it can be further verified that

$$\begin{aligned} &\alpha\theta_3\sum_{i=1}^{n}\left(\lambda_{\min}(H)\bar{\mu}_{i,3}^2\right)^{\frac{2-\xi}{2}} + \alpha\theta_3\sum_{i=1}^{n}\left(\lambda_{\min}(H)\bar{\mu}_{i,3}^2\right)^{\frac{2+\xi}{2}} \\ &- \alpha\sum_{i=1}^{n}\bar{\mu}_{i,3}(\bar{\mu}_i + h\bar{\mu}_i^5) \\ \le &\frac{\alpha}{2}\sum_{i=1}^{n}\left(\theta_3^2\lambda_{\min}^{2-\xi}(H) + \bar{\mu}_{i,3}^{2(2-\xi)}\right) \\ &+ \frac{\alpha}{2}\sum_{i=1}^{n}\left(\theta_3^2\lambda_{\min}^{2+\xi}(H) + \bar{\mu}_{i,3}^{2(2+\xi)}\right) - \alpha\sum_{i=1}^{n}\bar{\mu}_{i,3}(\bar{\mu}_{i,3}+\theta_3) \\ &- \alpha\sum_{i=1}^{n}\bar{\mu}_{i,3}h(\bar{\mu}_{i,3}+\theta_3)^5 = \alpha n\bar{\Pi}_3 \triangleq \Pi_3. \end{aligned}$$

Thus, (26) can be further calculated as

$$\begin{aligned} \dot{V}_3 \le &-\alpha\theta_3\sum_{i=1}^{n}|z_i|^{2-\xi} - \alpha\theta_3\sum_{i=1}^{n}\left(\lambda_{\min}(H)\bar{\mu}_{i,3}^2\right)^{\frac{2-\xi}{2}} \\ &- \alpha\theta_3\sum_{i=1}^{n}|z_i|^{2+\xi} - \alpha\theta_3\sum_{i=1}^{n}\left(\lambda_{\min}(H)\bar{\mu}_{i,3}^2\right)^{\frac{2+\xi}{2}} + \Pi_3 \\ \le &-\alpha\theta_3\left(\sum_{i=1}^{n}\left(z_i^2 + \lambda_{\min}(H)\bar{\mu}_{i,3}^2\right)\right)^{\frac{2-\xi}{2}} \\ &- \alpha\theta_3(2n)^{-\frac{\xi}{2}}\left(\sum_{i=1}^{n}\left(z_i^2 + \lambda_{\min}(H)\bar{\mu}_{i,3}^2\right)\right)^{\frac{2+\xi}{2}} + \Pi_3 \\ \le &-\alpha\theta_3\left(2\lambda_{\min}(H)V_3\right)^{\frac{2-\xi}{2}} \\ &- \alpha\theta_3(2n)^{-\frac{\xi}{2}}\left(2\lambda_{\min}(H)V_3\right)^{\frac{2+\xi}{2}} + \Pi_3. \end{aligned}$$

Since $\theta_3 = (2n)^{\frac{\xi}{4}}/(2\lambda_{\min}(H))$, by using Lemma 2, one can obtain that the frequency of DGs converges into the set of

$$\Omega_3 = \left\{\omega\middle| V_3 \le \frac{\Pi_3}{2(1-\varepsilon_3)\alpha}\right\}$$

in fixed time T_3^* bounded by

$$T_3^* \le \frac{\pi}{\varepsilon_3\xi\alpha}.$$

One further obtains that the FR error converges into the set of

$$\Omega_3^e = \left\{e\middle| e^Te \le \frac{\Pi_3}{\lambda_{\min}(H)(1-\varepsilon_3)\alpha}\right\}$$

in fixed time T_3^*. From the above analysis, we can conclude that practical fixed-time FR is achieved for DGs by using fully distributed controller (18)–(19). Next, we prove that practical fixed-time APS is realized among DGs.

Let $\bar{\nu}_{i,4} = \bar{\nu}_{ij} - \theta_4$, $i = 1, 2, \ldots, n$. From (23), the time derivative of V_4 can be calculated as

$$\begin{aligned} \dot{V}_4 = &\sum_{i=1}^{n}\epsilon_i\dot{\epsilon}_i + \sum_{i=1}^{n}\sum_{j=1}^{n}\dot{\bar{\nu}}_{ij}(\bar{\nu}_{ij}-\theta_4) \\ = &-\alpha\sum_{i=1}^{n}\epsilon_i\left(\sum_{j=1}^{n}a_{ij}\bar{\nu}_{ij}\mathrm{sig}^{1-\xi}(\epsilon_i-\epsilon_j)\right) \\ &- \alpha\sum_{i=1}^{n}\epsilon_i\left(\sum_{j=1}^{n}a_{ij}\bar{\nu}_{ij}\mathrm{sig}^{1+\xi}(\epsilon_i-\epsilon_j)\right) \\ &+ \sum_{i=1}^{n}\sum_{j=1}^{n}\bar{\nu}_{i,4}\left(\frac{\alpha}{2}a_{ij}|m_iP_i - m_jP_j|^{2-\xi}\right. \\ &\left. + \frac{\alpha}{2}a_{ij}|m_iP_i - m_jP_j|^{2+\xi} - \frac{\alpha}{2}\bar{\nu}_{ij} - \frac{\alpha}{2}h\bar{\nu}_{ij}^5\right) \\ = &-\frac{\alpha}{2}\sum_{i=1}^{n}\sum_{j=1}^{n}a_{ij}\bar{\nu}_{ij}|\epsilon_i-\epsilon_j|^{2-\xi} - \frac{\alpha}{2}\sum_{i=1}^{n}\sum_{j=1}^{n}a_{ij}\bar{\nu}_{ij}|\epsilon_i-\epsilon_j|^{2+\xi} \\ &+ \sum_{i=1}^{n}\sum_{j=1}^{n}\bar{\nu}_{i,4}\left(\frac{\alpha}{2}a_{ij}|\epsilon_i-\epsilon_j|^{2-\xi} + \frac{\alpha}{2}a_{ij}|\epsilon_i-\epsilon_j|^{2+\xi}\right. \\ &\left. - \frac{\alpha}{2}\bar{\nu}_{ij} - \frac{\alpha}{2}h\bar{\nu}_{ij}^5\right) \\ = &-\frac{\alpha\theta_4}{2}\sum_{i=1}^{n}\sum_{j=1}^{n}a_{ij}|\epsilon_i-\epsilon_j|^{2-\xi} - \frac{\alpha\theta_4}{2}\sum_{i=1}^{n}\sum_{j=1}^{n}a_{ij}|\epsilon_i-\epsilon_j|^{2+\xi} \\ &- \frac{\alpha\theta_4}{2}\sum_{i=1}^{n}\sum_{j=1}^{n}\left(2\lambda_2(\bar{L})\bar{\nu}_{i,4}^2\right)^{\frac{2-\xi}{2}} \\ &+ \frac{\alpha\theta_4}{2}\sum_{i=1}^{n}\sum_{j=1}^{n}\left(2\lambda_2(\bar{L})\bar{\nu}_{i,4}^2\right)^{\frac{2-\xi}{2}} \\ &- \frac{\alpha\theta_4}{2}\sum_{i=1}^{n}\sum_{j=1}^{n}\left(2\lambda_2(\tilde{L})\bar{\nu}_{i,4}^2\right)^{\frac{2+\xi}{2}} \\ &+ \frac{\alpha\theta_4}{2}\sum_{i=1}^{n}\sum_{j=1}^{n}\left(2\lambda_2(\tilde{L})\bar{\nu}_{i,4}^2\right)^{\frac{2+\xi}{2}} \\ &- \frac{\alpha}{2}\sum_{i=1}^{n}\sum_{j=1}^{n}\bar{\nu}_{i,4}(\bar{\nu}_{ij} + h\bar{\nu}_{ij}^5). \end{aligned} \tag{27}$$

It can be verified that

$$\begin{aligned} &\alpha\theta_4\left(2\lambda_2(\bar{L})\bar{\nu}_{i,4}^2\right)^{\frac{2-\xi}{2}} + \alpha\theta_4\left(2\lambda_2(\tilde{L})\bar{\nu}_{i,4}^2\right)^{\frac{2+\xi}{2}} - \alpha\bar{\nu}_{i,4}(\bar{\nu}_{ij} + h\bar{\nu}_{ij}^5) \\ \le &\alpha\left(\frac{(h\theta_4^5+\theta_4)^2}{20h^2\theta_4^4} + \frac{5^5(5h\theta_4)^6}{6(6(h-1))^5} + \frac{3^3(10h\theta_4^3)^4}{4(40h\theta_4^2)^3}\right. \\ &\left. + \frac{1}{2}\theta_4^2 2^{2-\xi}\lambda_2^{2-\xi}(\bar{L}) + \frac{1}{2}\theta_4^2 2^{2+\xi}\lambda_2^{2+\xi}(\tilde{L})\right) = \alpha\bar{\Pi}_4. \end{aligned}$$

Let $\Pi_4 = \alpha n\bar{\Pi}_4$. Then, (27) can be further calculated as

$$\begin{aligned} V_4 \le &-\frac{\alpha\theta_4}{2}\sum_{i=1}^{n}\sum_{j=1}^{n}a_{ij}|\epsilon_i-\epsilon_j|^{2-\xi} - \frac{\alpha\theta_4}{2}\sum_{i=1}^{n}\sum_{j=1}^{n}a_{ij}|\epsilon_i-\epsilon_j|^{2+\xi} \\ &- \frac{\alpha\theta_4}{2}\sum_{i=1}^{n}\sum_{j=1}^{n}\left(2\lambda_2(\bar{L})\bar{\nu}_{i,4}^2\right)^{\frac{2-\xi}{2}} \\ &- \frac{\alpha\theta_4}{2}\sum_{i=1}^{n}\sum_{j=1}^{n}\left(2\lambda_2(\tilde{L})\bar{\nu}_{i,4}^2\right)^{\frac{2+\xi}{2}} + \Pi_4 \\ \le &-\frac{\alpha\theta_4}{2}\left(\sum_{i=1}^{n}\sum_{j=1}^{n}\left(a_{ij}^{\frac{2}{2-\xi}}(\epsilon_i-\epsilon_j)^2 + 2\lambda_2(\bar{L})\bar{\nu}_{i,4}^2\right)\right)^{\frac{2-\xi}{2}} \end{aligned}$$

$$
\begin{aligned}
&-\frac{\alpha\theta_4}{2}(2n^2)^{-\frac{\xi}{2}}\Bigg(\sum_{i=1}^{n}\sum_{j=1}^{n}\Big(a_{ij}^{\frac{2}{2+\xi}}(\epsilon_i-\epsilon_j)^2\\
&\qquad+2\lambda_2(\tilde{L})\bar{v}_{i,4}^2\Big)\Bigg)^{\frac{2+\xi}{2}}+\Pi_4\\
&\le-\frac{\alpha\theta_4}{2}\Big(4\lambda_2(\bar{L})V_4\Big)^{\frac{2-\xi}{2}}-\frac{\alpha\theta_4}{2}(2n^2)^{-\frac{\xi}{2}}\Big(4\lambda_2(\tilde{L})V_4\Big)^{\frac{2+\xi}{2}}+\Pi_4\\
&\le-\frac{\alpha\theta_4}{2}\Big(4\underline{\lambda}_2V_4\Big)^{\frac{2-\xi}{2}}-\frac{\alpha\theta_4}{2}(2n^2)^{-\frac{\xi}{2}}\Big(4\underline{\lambda}_2V_4\Big)^{\frac{2+\xi}{2}}+\Pi_4.
\end{aligned}
$$

Since $\theta_4=(2n^2)^{\frac{\xi}{4}}/(2\underline{\lambda}_2)$, by using Lemma 2, one can obtain that the APS of DGs converges into the set of

$$\Omega_4=\left\{P\middle|V_4\le\frac{\Pi_4}{2(1-\varepsilon_4)\alpha}\right\}$$

in fixed time T_4^* bounded by

$$T_4^*\le\frac{\pi}{\varepsilon_4\xi\alpha}.$$

One further obtains that the APS error converges into the set of

$$\Omega_4^\epsilon=\left\{\epsilon\middle|\epsilon^T\epsilon\le\frac{\Pi_4}{(1-\varepsilon_4)\alpha}\right\}$$

in fixed time T_4^*. Hence, practical fixed-time APS is realized among DGs by using fully distributed controller (20)–(21).

Remark 1. A finite-time controller is developed to realize frequency restoration of DGs in finite time (Zuo et al., 2016). Considering external disturbances, a robust finite-time controller is proposed (Dehkordi et al., 2017a). Furthermore, finite-time controllers are designed with switching topology or communication delays (Ning et al., 2021; Wang et al., 2017). However, the settling time is not explicitly estimated (Dehkordi et al., 2017a; Wang et al., 2017) or is depending on global topology information (Ning et al., 2021; Zuo et al., 2016). For example, the controllers proposed in Zuo et al. (2016) are in the form of

$$u_{i,\omega}=\alpha\Big(\sum_{j\in\mathcal{N}_i}a_{ij}\mathrm{sig}^{\xi}(\omega_j-\omega_i)+b_i\mathrm{sig}^{\xi}(\omega_r-\omega_i)\Big),\tag{28}$$

$$u_{i,P}=\alpha\sum_{j\in\mathcal{N}_i}a_{ij}\mathrm{sig}^{\xi}(m_jP_j-m_iP_i),\tag{29}$$

by using which the derived settling time depends on global topology information. Note that fixed gains are used in Dehkordi et al. (2017a), Ning et al. (2021), Wang et al. (2017), Zuo et al. (2016), e.g., α in (28). Instead, in this paper the proposed fully distributed fixed-time controllers exploit adaptive control gains, e.g., $\bar{\mu}_i$ in (18)–(19), guaranteeing that an explicit settling time bound is derived, which is independent of global topology information and the total number of DGs in the microgrid. Moreover, the controller itself, e.g., controller (18)–(19), is independent of global topology information and the total DG number n. Therefore, the proposed fully distributed control scheme is ready to be applied to large-scale systems. As a trade-off, the FR error and the APS error will not converge to zero but to the neighborhood of zero. The size of the error set can be adjusted through different communication graph patterns and different parameters. For example, the size of Ω_1^e in Theorem 1 will be reduced if the communication graph is well-connected (i.e., a larger $\lambda_{\min}(H)$ with high connectivity) and/or utilizing a smaller ε_1.

5. Case studies

In this section, based on a modified IEEE 34-bus test system (Bidram et al., 2014), i.e., in Fig. 2, case studies are conducted on a test system consisting of five DGs and three loads. The communication graph together with communication strength is shown in Fig. 3. The frequency reference level is only available to DG 4.

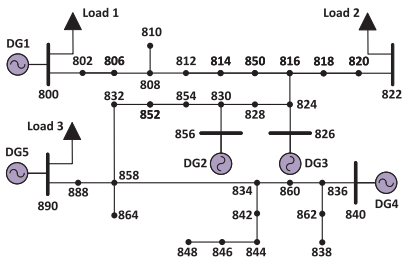

Fig. 2. The modified IEEE 34 bus test feeder.

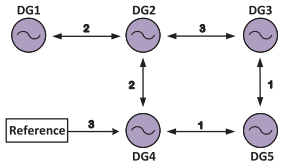

Fig. 3. Communication topology among DGs.

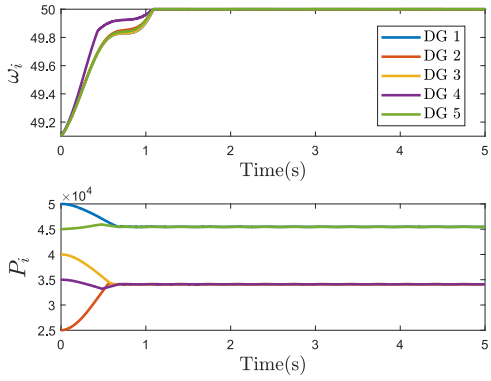

Fig. 4. Performance using fully distributed finite-time controllers (7)–(10).

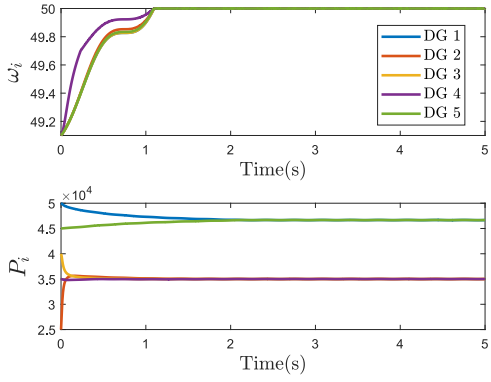

Fig. 5. Performance using fully distributed fixed-time controllers (18)–(21).

5.1. Performance evaluation

The reference level for frequency is 50 Hz. The droop coefficients are set as $m_1=m_5=14.1\times10^{-5}$, $m_2=m_3=m_4=18.8\times10^{-5}$. Other used parameters of line impedances are refereed to Bidram et al. (2014). At $t=0$ s, the test system

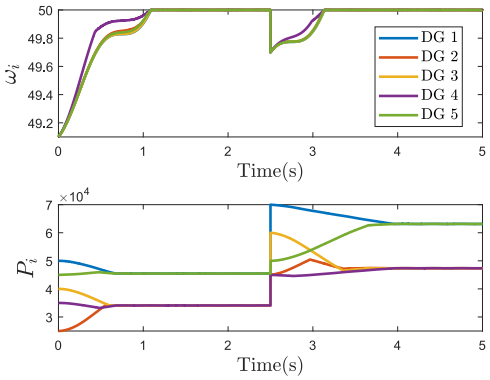

Fig. 6. Robustness to load changes using fully distributed finite-time controllers.

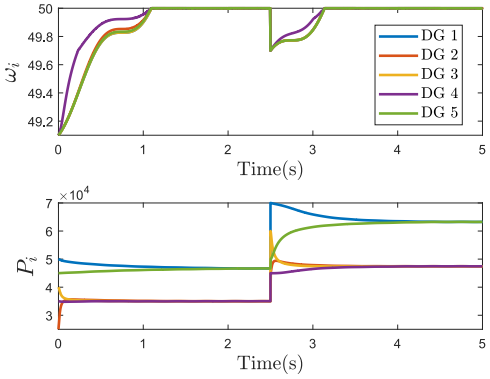

Fig. 7. Robustness to load changes using fully distributed fixed-time controllers.

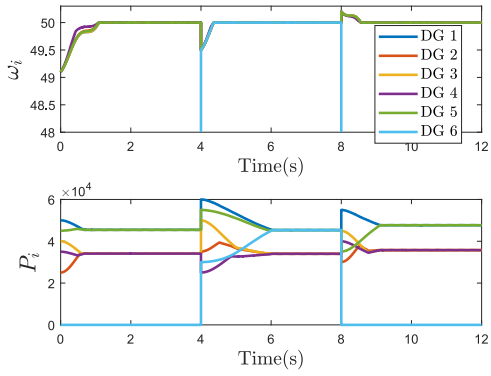

Fig. 8. Plug-and-play capability using fully distributed finite-time controllers.

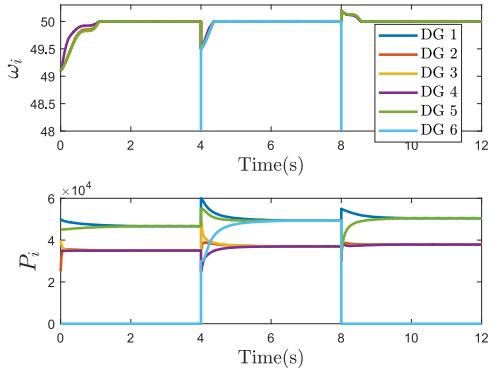

Fig. 9. Plug-and-play capability using fully distributed fixed-time controllers.

is initialized with $\omega_1(0) = \omega_2(0) = \omega_3(0) = \omega_4(0) = \omega_5(0) = 49.1$ Hz, $P_1(0) = 50$ KW, $P_2(0) = 25$ KW, $P_3(0) = 40$ KW, $P_4(0) = 35$ KW, and $P_5(0) = 45$ KW. External disturbances are $\zeta_i^{\omega}(t) = 0.8\sin(2\pi t)$, $i = 1, 2, 3, 4, 5$. The controller parameters are selected as: $\alpha = 1$, $k_1 = k_2 = 0.8$, $\xi = 0.2$, and $h = 1.2$.

Applying fully distributed finite-time controllers described by (7)–(10) with $n = 5$, results are shown in Fig. 4, where frequency of DGs is restored to the reference level at $t = 1.2$ s, and APS among DGs is achieved at $t = 0.7$ s. Then, applying fully distributed fixed-time controllers described by (18)–(21) with $n = 5$, results are shown in Fig. 5, where frequency of DGs is restored to the reference level at $t = 1.2$ s, and APS among DGs is achieved at $t = 2.0$ s. The convergence is usually faster when using fixed-time controllers than finite-time ones (Ning et al., 2023). However, as shown in Figs. 4 and 5, it takes more time to realize APS when using the fully distributed fixed-time controller than the finite-time counterpart. The slower convergence is caused by the adaptive term in (21), which can increase slower than that in (10). This comparison implies the difference between our proposed fully distributed secondary controllers and conventional ones. Although the convergence speed is compromised to some extent by using the fully distributed controller, its capability to apply to a large-scale islanded microgrids is promising without using global topology information.

5.2. Robustness to load changes

5.3. Accelerated convergence through comparison

Loads can change in microgrids based on different user requirement. Therefore, it is an important task to validate the robustness of the proposed fully-distributed controllers against load changes. Without loss of generality, we consider that Load 2 is doubled at $t = 2.5$ s. Applying the fully distributed finite-time and fixed-time controllers with $n = 5$, results are shown in Figs. 6 and 7, respectively. It is observed that, at $t = 2.5$ s the frequency and the active power encounter some deviations caused by the load change from Load 2, then the frequency is restored within 3.2 s and the APS is achieved within 3.8 s. Therefore, it is demonstrated that the proposed fully distributed controllers are robust against load changes.

5.4. Plug-and-play capability

Due to the intermittent nature of DGs in a microgrid, it is necessary to validate that, when some DGs are plugged into or out of the microgrid, the proposed fully distributed controllers are still effective to ensure the whole system operate in a normal mode. To address this concern, we consider that a "DG 6" is added to Bus 838 of the microgrid at $t = 4$ s, and is later removed at $t = 8$ s. Meanwhile, it is assumed that DG 6 is a neighbor of DG 4 with communication strength 2 for 4 s $\leq t \leq$ 8 s on top of the existing topology in Fig. 3. Applying the proposed fully distributed controllers, results are shown in Figs. 8 and 9, respectively. We can observe that, at $t = 4$ s, the frequency and the active power of DGs encounter some deviations due to the addition of DG 6, then the frequency is restored within 4.6 s and APS is achieved within 6.0 s. Once DG 6 is plugged out from the microgrid, the frequency and the active power again encounter some deviations before returning to the reference level and achieving APS, respectively.

Besides the fully distributed feature of our proposed controllers, another promising feature is the accelerated convergence of FR and APS in islanded microgrids. In order to make a comparison, a fully distributed controller with asymptotic convergence

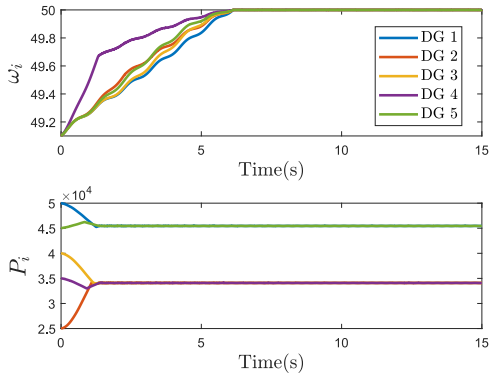

Fig. 10. Comparison results using fully distributed finite-time controllers (7)–(10).

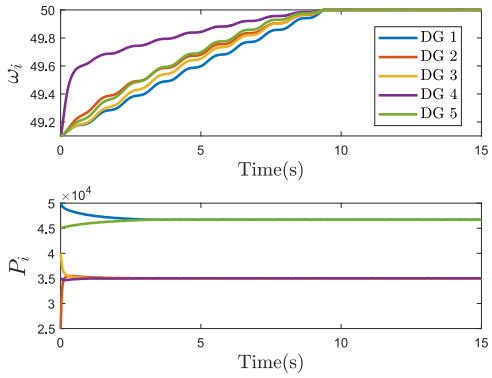

Fig. 11. Comparison results using fully distributed fixed-time controllers (18)–(21).

is presented for DG i, $i \in \Omega$, as:

$$u_i^{\omega} = -\tilde{\mu}_i \alpha \left(\sum_{j \in \mathcal{N}_i} a_{ij}(\omega_i - \omega_j) + b_i(\omega_i - \omega_{\mathrm{r}}) \right) - k_3 \mathrm{sign}\left(\sum_{j \in \mathcal{N}_i} a_{ij}(\omega_i - \omega_j) + b_i(\omega_i - \omega_{\mathrm{r}}) \right), \tag{30}$$

$$\dot{\tilde{\mu}}_i = \alpha \left(\sum_{j \in \mathcal{N}_i} a_{ij}(\omega_i - \omega_j) + b_i(\omega_i - \omega_{\mathrm{r}}) \right)^2 - \alpha \tilde{\mu}_i, \tag{31}$$

where $\tilde{\mu}_i$ is an adaptive gain with $\tilde{\mu}_i(0) > 0$, and $k_3 \geq d$.

In order to realize APS, a fully distributed controller with asymptotic convergence is further provided for DG i, $i \in \Omega$, as:

$$u_i^{P} = -\alpha \sum_{j \in \mathcal{N}_i} a_{ij} \tilde{\nu}_{ij}(m_i P_i - m_j P_j), \tag{32}$$

$$\dot{\tilde{\nu}}_{ij} = \frac{\alpha}{2} a_{ij} |m_i P_i - m_j P_j|^2 - \frac{\alpha}{2} \tilde{\nu}_{ij}, \tag{33}$$

where $\tilde{\nu}_{ij}$ is an adaptive gain with $\tilde{\nu}_{ij} = \tilde{\nu}_{ji}$ and $\tilde{\nu}_{ij}(0) > 0$.

External disturbances considered in this section are $\zeta_i^{\omega}(t) = 0.08\sin(2\pi t)$, $i = 1, 2, 3, 4, 5$. The controller parameters are selected as: $\alpha = 0.5$, $k_1 = k_2 = k_3 = 0.08$. Other unmentioned parameters keep the same as those in Section 5.1. With $n = 5$, applying fully distributed finite-time controllers described by (7)–(10), fully distributed fixed-time controllers described by (18)–(21), and fully distributed asymptotic controllers described by (30)–(33), results are shown in Figs. 10–12, where frequency of DGs is restored to the reference level at $t = 6.1$ s, $t = 9.3$ s, and $t = 10.7$ s, respectively, and APS among DGs is achieved at $t = 1.3$ s, $t = 3.2$ s, and $t = 5.7$ s, respectively. Therefore, our proposed controllers accelerate the convergence of FR and APS in islanded microgrids.

6. Conclusion

This paper has investigated the accelerated secondary FR and APS in islanded microgrids. Fully distributed finite-time controllers have been proposed to ensure that the FR error and the APS error are converged to adjustable sets in finite-time. To further lift the restrictions of the dependance on initial conditions, fully distributed fixed-time controllers have been proposed. Both type of proposed controllers do not depend on global information of communication topology. The developed fully distributed control scheme has the potential of becoming a promising solution for the resilient and efficient management of large-scale islanded microgrids. The effectiveness of the proposed approach has been validated through extensive simulations on a modified IEEE 34 bus test feeder, demonstrating superior performance in terms of FR, APS, and transient response under various operating conditions and disturbance scenarios. Future work will concentrate on designing smooth fully distributed controllers without using the sign function. Another interesting direction is to design fully distributed controllers for voltage regulation and reactive power sharing.

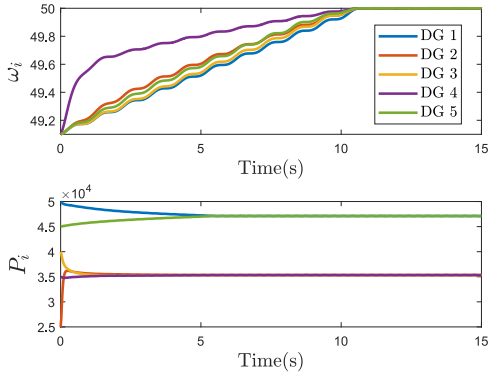

Fig. 12. Comparison results using fully distributed asymptotic controllers (30)–(33).

References

Bhat, S. P., & Bernstein, D. S. (2000). Finite-time stability of continuous autonomous systems. *SIAM Journal on Control and Optimization*, *38*(3), 751–766.

Bidram, A., Davoudi, A., & Lewis, F. L. (2014). A multiobjective distributed control framework for islanded AC microgrids. *IEEE Transactions on Industrial Informatics*, *10*(3), 1785–1798.

Bidram, A., Davoudi, A., Lewis, F. L, & Guerrero, J. M. (2013). Distributed cooperative secondary control of microgrids using feedback linearization. *IEEE Transactions on Power Systems*, *28*(3), 3462–3470.

Cao, L., Xiao, B., Golestani, M., & Ran, D. (2020). Faster fixed-time control of flexible spacecraft attitude stabilization. *IEEE Transactions on Industrial Informatics*, *16*(2), 1281–1290.

Chen, F., Chen, M., Li, Q., Meng, K., Zheng, Y., Guerrero, J. M., & Abbott, D. (2017). Cost-based droop schemes for economic dispatch in islanded microgrids. *IEEE Transactions on Smart Grid*, *8*(1), 63–74.

Chen, G., & Guo, Z. (2019). Distributed secondary and optimal active power sharing control for islanded microgrids with communication delays. *IEEE Transactions on Smart Grid*, *10*(2), 2002–2014.

Dehkordi, N. M., Sadati, N., & Hamzeh, M. (2017a). Distributed robust finite-time secondary voltage and frequency control of islanded microgrids. *IEEE Transactions on Power Systems*, *32*(5), 3648–3659.

Dehkordi, N. M., Sadati, N., & Hamzeh, M. (2017b). Fully distributed cooperative secondary frequency and voltage control of islanded microgrids. *IEEE Transactions on Energy Conversion*, *32*(2), 675–685.

Ding, L., Han, Q.-L., & Zhang, X.-M. (2019). Distributed secondary control for active power sharing and frequency regulation in islanded microgrids using an event-triggered communication mechanism. *IEEE Transactions on Industrial Informatics*, *15*(7), 3910–3922.
Guerrero, J. M., Vasquez, J. C., Matas, J., de Vicuna, L. G., & Castilla, M. (2011). Hierarchical control of droop-controlled AC and DC microgrid–a general approach toward standardization. *IEEE Transactions on Industrial Electronics*, *58*(1), 158–172.
Guo, F., Wen, C., Mao, J., & Song, Y.-D. (2015). Distributed secondary voltage and frequency restoration control of droop-controlled inverter-based microgrids. *IEEE Transactions on Industrial Electronics*, *62*(7), 4355–4364.
Krstic, M., Kanellakopoulos, I., & Kokotovic, P. V. (1995). *Nonlinear and adaptive control design*. Wiley.
Li, Q., Chen, F., Chen, M., Guerrero, J. M., & Abbott, D. (2016). Agent-based decentralized control method for islanded microgrids. *IEEE Transactions on Smart Grid*, *7*(2), 637–649.
Li, Z., Wen, G., Duan, Z., & Ren, W. (2015). Designing fully distributed consensus protocols for linear multi-agent systems with directed graphs. *IEEE Transactions on Automatic Control*, *60*(4), 1152–1157.
Ning, B., Han, Q.-L., & Ding, L. (2021). Distributed finite-time secondary frequency and voltage control for islanded microgrids with communication delays and switching topologies. *IEEE Transactions on Cybernetics*, *51*(8), 3988–3999.
Ning, B., Han, Q.-L., Zuo, Z., Ding, L., Lu, Q., & Ge, X. (2023). Fixed-time and prescribed-time consensus control of multi-agent systems and its applications: A survey of recent trends and methodologies. *IEEE Transactions on Industrial Informatics*, *19*(2), 1121–1135.
Ning, B., Jin, J., Zheng, J., & Man, Z. (2018). Finite-time and fixed-time leader-following consensus for multi-agent system. *International Journal of Control*, *91*(6), 1259–1270.
Simpson-Porco, J. W., Shafiee, Q., Dorfler, F., Vasquez, J. C., & Guerrero, J. M. (2015). Secondary frequency and voltage control of islanded microgrids via distributed averaging. *IEEE Transactions on Industrial Electronics*, *62*(11), 7025–7038.
Tan, K. T., Peng, X. Y., So, P. L., Chu, Y. C., & Chen, M. Z. Q. (2012). Centralized control for parallel operation of distributed generation inverters in microgrids. *IEEE Transactions on Smart Grid*, *3*(4), 1977–1987.
Wang, X., Zhang, H., & Li, C. (2017). Distributed finite-time cooperative control of droop-controlled microgrids under switching topology. *IET Renewable Power Generation*, *11*(5), 707–714.
Xu, Y., & Sun, H. (2018). Distributed finite-time convergence control of an islanded low-voltage AC microgrid. *IEEE Transactions on Power Systems*, *33*(3), 2339–2348.
Yu, S., & Long, X. (2015). Finite-time consensus for second-order multi-agent systems with disturbances by integral sliding mode. *Automatica*, *54*, 158–165.
Zhao, D., Zhang, C., Sun, Y., Li, S., Sun, B., & Li, Y. (2021). Distributed robust frequency restoration and active power sharing for autonomous microgrids with event-triggered strategy. *IEEE Transactions on Smart Grid*, *12*(5), 3819–3834.
Zhou, Q., Shahidehpour, M., Yan, M., Wu, X., Alabdulwahab, A., & Abusorrah, A. (2020). Distributed secondary control for islanded microgrids with mobile emergency resources. *IEEE Transactions on Power Systems*, *35*(2), 1389–1399.
Zhu, Z., Xia, Y., & Fu, M. (2011). Attitude stabilization of rigid spacecraft with finite-timeconvergence. *International Journal of Robust and Nonlinear Control*, *21*, 686–702.
Zuo, S., Davoudi, A., Song, Y., & Lewis, F. L. (2016). Distributed finite-time voltage and frequency restoration in islanded AC microgrids. *IEEE Transactions on Industrial Electronics*, *63*(10), 5988–5997.

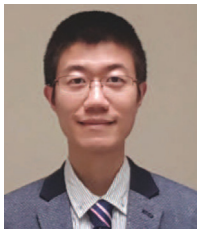

Boda Ning received the B.Eng. degree in automatic control from East China University of Science and Technology, Shanghai, China, in 2011, the M.Sc. degree (with Distinction) in control systems from University of Manchester, Manchester, U.K., in 2012, and the Ph.D. degree in electrical and electronic engineering from Swinburne University of Technology, Melbourne, Australia, in 2017.

He is currently a Senior Lecturer (tenured) at Department of Electrical and Electronic Engineering with Auckland University of Technology, Auckland, New Zealand. From September 2017 to October 2024, he held various academic positions such as Research Fellow and Senior Research Engineer with Swinburne University of Technology and RMIT University, Melbourne, Australia.

Dr Ning's research interest includes cooperative control of multi-agent systems and its application to intelligent robotics, smart grids, and intelligent vehicles.

Qing-Long Han received the B.Sc. degree in Mathematics from Shandong Normal University, Jinan, China, in 1983, and the M.Sc. and Ph.D. degrees in Control Engineering from East China University of Science and Technology, Shanghai, China, in 1992 and 1997, respectively.

Professor Han is currently Pro Vice-Chancellor (Research Quality) and a Distinguished Professor at Swinburne University of Technology, Melbourne, Australia. He held various academic and management positions at Griffith University and Central Queensland University, Australia. His research interests include networked control systems, multi-agent systems, time-delay systems, smart grids, unmanned surface vehicles, and neural networks.

Professor Han was awarded the 2024 IEEE Dr.-Ing. Eugene Mittelmann Achievement Award (the Highest Award in Industrial Electronics), the 2021 Norbert Wiener Award (the Highest Award in Systems Science and Engineering, and Cybernetics) and the 2021 M. A. Sargent Medal (the Highest Award of the Electrical College Board of Engineers Australia). He was the recipient of the IEEE Systems, Man, and Cybernetics Society Andrew P. Sage Best Transactions Paper Award in 2022, 2020, and 2019, respectively, the IEEE/CAA Journal of Automatica Sinica Norbert Wiener Review Award in 2020, and the IEEE Transactions on Industrial Informatics Outstanding Paper Award in 2020.

Professor Han is a Member of the Academia Europaea (The Academy of Europe). He is a Fellow of the International Federation of Automatic Control (FIFAC), a Fellow of the Institute of Electrical and Electronics Engineers (FIEEE), an Honorary Fellow of the Institution of Engineers Australia (HonFIEAust), and a Fellow of the Chinese Association of Automation (FCAA). He is a Highly Cited Researcher in both Engineering and Computer Science (Clarivate). He has served as an AdCom Member of IEEE Industrial Electronics Society (IES), a Member of IEEE IES Fellows Committee, a Member of IEEE IES Publications Committee, Chair of IEEE IES Technical Committee on Network-Based Control Systems and Applications, and the Co-Editor-in-Chief of IEEE Transactions on Industrial Informatics. He is currently the Editor-in-Chief of IEEE/CAA Journal of Automatica Sinica and the Co-Editor of Australian Journal of Electrical and Electronic Engineering.

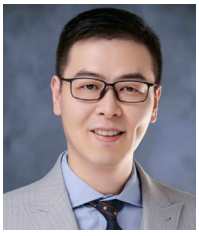

Zongyu Zuo received his B.Eng. degree in Automatic Control from Central South University, Hunan, China, in 2005, and Ph.D. degree in Control Theory and Applications from Beihang University (BUAA), Beijing, China, in 2011.

He was an academic visitor at the School of Electrical and Electronic Engineering, University of Manchester from September 2014 to September 2015 and held an inviting associate professorship at Mechanical Engineering and Computer Science, UMR CNRS 8201, Université de Valenciennes et du Hainaut-Cambrésis in October 2015 and May 2017. He is currently a full professor at the School of Automation Science and Electrical Engineering, Beihang University. His research interests are in the fields of nonlinear system control, control of UAVs, and coordination of multi-agent system.

Prof. Zuo currently serves as an Associate Editor for IEEE Transactions on Industrial Informatics, IEEE/CAA Journal of Automatica Sinica, Journal of The Franklin Institute, Journal of Vibration and Control, and International Journal of Aeronautical & Space Sciences. He was identified as a Highly Cited Researcher by Clarivate Analytics as well as a most cited Chinese Researcher by Elsevier.

Lei Ding received the B.Eng. degree in Automation, and the M.Eng. and Ph.D. degrees in Control Theory and Control Engineering from the Dalian Maritime University, Dalian, China, in 2007, 2009, and 2014, respectively. From 2015 to 2016, he was a Visiting Research Fellow with Western Sydney University, Australia. From 2016 to 2017, he was a Postdoctoral Associate with Wayne State University, USA. From 2017 to 2019, he worked as a Research Fellow with the Swinburne University of Technology, Australia. He is currently a Full Professor at the Nanjing University of Posts and Telecommunications, Nanjing, China. His research interests include cooperative control of networked systems, smart grid, distributed optimization and game theory.

Professor Ding was the recipient of the 2021 IEEE/CAA Journal of Automatica Sinica Norbert Wiener Review Award, the 2020 IEEE Transactions on Industrial Informatics Outstanding Paper Award, and the 2019 IEEE Systems, Man, and Cybernetics (SMC) Society Andrew P. Sage Best Transactions Paper Award (IEEE Transactions on Cybernetics). He is an Associate Editor of IEEE Transactions on Industrial Informatics and IEEE/ CAA Journal of Automatica.